01

Emission spectra of low-pressure air during a diffuse streamer discharge

© B.F. Tarasenko, E.Kh. Baksht, N.P. Vinogradov, D.A. Sorokin

Institute of High Current Electronics, Siberian Branch, Russian Academy of Sciences,
634055 Tomsk, Russia

e-mail: vft@loi.hcei.tsc.ru, beh@loi.hcei.tsc.ru, vinikitavin@mail.ru, SDmA-70@loi.hcei.tsc.ru

Received 11.08.2022
Revised 16.09.2022
Accepted 29.09.2022

Attention to the study of the radiation characteristics of streamer discharges in atmospheric air at pressures of a fraction of a Torr unit is primarily associated with obtaining new data on high-altitude discharges, including red sprites. This paper presents the results of studying the characteristics of the radiation of a streamer discharge in low-pressure air upon initiation of ionization waves (streamers) by a repetitively pulsed barrier discharge. It has been established that at air pressures of $\Delta p = 0.08-3$ Torr, the lines of the second positive, first negative, and first positive nitrogen systems have the highest intensities in the wavelength range of $\Delta\lambda = 280-900$ nm, and their contribution to the spectral radiation energy density depends on the discharge region and pressure. The emission bands of the first positive nitrogen system give the red color of the ionization waves, however, the highest intensities under these conditions are recorded on the lines of the second positive and first negative nitrogen systems. It is shown that when the pressure decreases to 0.04 Torr or less, the spectrum and color of the streamer discharge, while maintaining the amplitude of the voltage pulses, changes significantly. New lines and bands appear in it, including intense lines of atomic hydrogen, which is due to an increase in the reduced electric field strength, respectively, in the electron temperature. This leads to the dissociation of molecular gases that are part of the air, as well as those adsorbed by the chamber walls.

Keywords: emission spectra, streamer discharge, air, low pressures.

DOI: 10.21883/EOS.2022.12.55234.4014-22

Introduction

Studies of high-altitude electrical discharges, which are called transient light phenomena (TLP) [1,2], much attention has been paid in recent years. The scale of such electric discharge phenomena usually amounts to tens-hundreds of kilometers, and the color, shape and emission spectra of the TLP depend on the type of discharge and distance from the Earth's surface (altitude above sea level h). A significant number of studies are aimed at studying red sprites, which during thunderstorm activity are observed at altitudes of 40−100 km [1–15]. To study the processes that ensure the initiation and development of red sprites, aircraft [7,8], satellites are used [9] and the International Space Station [10]. The initiation of red sprites usually occurs at altitudes of 70−80 km, and the directions of their propagation are stochastic. Some images show red sprites in the form of straight channels extending both down (column sprites [14]) and down and up (currot sprites [14]) — accordingly, in the direction of increasing and decreasing air pressure p. At the same time, there is both a slight increase in their transverse dimensions (diameter) and a decrease, and there is also a decrease in the brightness of the glow (see, for example, the photos in Fig. 1 in [6] and in Fig. 2 in [11]). The appearance of red sprites is associated with the development of streamers (ionization waves) starting from areas in which plasma is formed with an increased concentration of charged particles [2,3]. The literature contains data on the speed of propagation of sprites, as well as the spectral composition of radiation and plasma parameters [1–15]. Nevertheless, the process of researching sprites is very complex and requires a lot of material costs. Therefore, along with the study of sprites, blue jets and other TLP in natural conditions, attempts are being made to simulate these phenomena in laboratory conditions. Various types of electric gas discharges are used for this, including glow [15] and apocampic [16,17]. In [15], it was reported that a glow discharge with a positive red column was ignited between two electrodes in a transparent tube filled with air at $p = 1.2$ Torr. The color of the discharge was determined by the radiation of the bands of the first positive (1+) molecular nitrogen system N_2 in the wavelength range $\Delta\lambda = 500-900$ nm.

Blue jets were simulated in [16,17] (bluejet [6,10]). In the works cited above, two electrodes with a small radius of curvature were placed inside a quartz tube at a distance of 1 cm relative to each other. It should be noted that in the areas of formation as red sprites [1–15], so blue and giant jets (blue and gigantic jets, Fig. 1 in [10]) there are no metal electrodes. Thus, the conditions under which the discharges were ignited in [15–17] are far from real for TLP. Therefore, in this work, as in recent works [18,19], a barrier pulse-periodic discharge was used to create a plasma initiating a phenomenon similar to atmospheric.

One of the important research tasks is to determine the excitation conditions under which a red-colored plasma

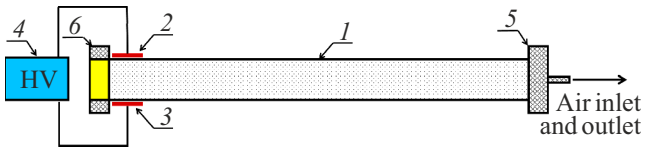

Figure 1. Installation for forming a streamer discharge: *1* — quartz tube; *2, 3* — aluminum foil electrodes; *4* — pulse high-voltage generator with variable polarity and adjustable voltage amplitude; *5* — caprolon flange with a nozzle for pumping and air intake; *6* — caprolon flange with a built-in quartz window.

of streamer discharges is realized in low-pressure air, as well as to study the spectral composition of the radiation of this plasma. At the same time, the air pressure should correspond to the pressures (more precisely, particle concentrations N) occurring at altitudes of 40–100 km, where the initiation (70–80 km) and the spread of sprites takes place [1–15].

The purpose of this work is to study the emission spectra of a plasma of a stimeric discharge in air at low p corresponding to those at which red sprites are observed. In addition, it is of interest to study the spectral composition of plasma radiation under conditions of its color changing from red to blue, which is observed at altitudes of 40–50 km when sprites propagate to the Earth's surface.

Experimental setup and measurement techniques

To ignite the streamer discharge at low pressures of air and other gases, an installation was created, the block diagram of which is shown in Fig. 1.

The discharge was ignited in a tube made of quartz of the GE-214 brand, which has a high transmittance in the ultraviolet (UV), visible and near infrared (IR) spectral regions. The length of the tube and its inner diameter were 120 cm and 5 cm, respectively. Flanges made of caprolon were attached to the ends of the tube. In the left (relative to the reader), a quartz window of the KU-1 brand was mounted, and in the right — a caprolon fitting through which the tube was pumped out and air was let into it from the laboratory room. The humidity in the room during the research was $\sim 23\%$. When receiving data for each set of conditions, the chamber was pumped out by a pre-vacuum pump to $p = 10^{-2}$ Torr, and then filled with air to the desired pressure.

To excite the discharge, a high-voltage generator was used, forming voltage pulses of positive or negative polarity with an adjustable amplitude. In most experiments, the frequency of repetition of voltage pulses was 21 kHz. When operating in idle mode, the amplitude of the voltage pulse generated by the generator was 7 kV with a half-height duration of $\sim 1.5\,\mu$s. The duration of the front and the decay of the voltage pulse were the same and equal to ~ 350 ns. The generator was connected to two electrodes made in the form of strips of aluminum foil with a length of 5 cm and a width of 1 cm. In contrast to the works [18,19] the electrodes had a different shape and were tightly attached to the surface of the quartz tube opposite each other at its left end.

The measurements were specially carried out at a high pulse repetition rate. This made it possible to photograph the glow of the discharge plasma and record its emission spectra at low specific energy deposits per pulse, which, according to estimates, coincided in order of magnitude with those realized in natural sprites. As known from the [1–15], the sizes of sprites range from hundreds of meters to tens of kilometers, and their glow, depending on the type and size of the sprite, lasts units-tens of milliseconds, which, with their relatively low specific luminosity, allows reliable photographing from long distances. In our experiments, in order to obtain high-quality photographs and radiation spectra, it is necessary to accumulate data for several thousand pulses. Previously, a similar technique was used to study the properties of apocampic discharge in various gases [16,17], as well as streamer discharge in air [18,19].

It should be noted that when measuring the pulse durations of natural discharges, a glow is usually recorded from the entire glow region of a sprite, which has dimensions of tens of kilometers in height and usually consists of a large number of plasma diffuse jets (streamers), which also occupy large sizes (tens of kilometers) in cross-section. In addition, individual „pillars“ and sprite branches start with different lag times [14]. In these experiments, using a pulse generator with a voltage of units of kilovolts at pressures corresponding to the air pressure in the area of sprite formation, single streamers with a length of about a meter were created. The duration of the pulses of radiation of streamer discharges, as is known, is mainly determined by the glow of the front of the streamer moving in space. Accordingly, the pulse durations should be compared when the sprite front and the plasma diffuse jet (PDJ) pass the same distances. In sprite, the glow of the streamer front will continue from the time of its initiation to the time of its attenuation at a distance of units-tens of kilometers from the initial region, which leads to an increase in the duration of the radiation pulses by several orders of magnitude. In addition, the duration of the sprite radiation pulses increases due to the formation of its separate „pillars “and branches that are not initiated simultaneously.

The voltage at the discharge gap was measured by means of an ACA-6039 divider (AKTAKOM), and the discharge current — by a shunt based on TVO brand resistors. The signals from the voltage divider and current shunt were recorded by a digital oscilloscope Tektronix MDO 3104 (1 GHz, 5 GS/s). Discharge plasma emission spectra were recorded using an HR2000+ES spectrometer (OceanOptics Inc.) equipped with a quartz light guide. The spectral sensitivity of the spectrometer and the transmission of the light guide in the range $\Delta\lambda = 190$–1100 nm are known. The resolution of the optical system was no worse than ~ 0.9 nm. Shooting of the integral glow of

Values of pressure p and particle concentrations N of air at various altitudes above sea level h

h, km	p, Torr	N, cm^{-3}
40	2.6	$9.5 \cdot 10^{16}$
47.4	1	$3.6 \cdot 10^{16}$
52.6	0.5	$1.9 \cdot 10^{16}$
60	0.2	$8 \cdot 10^{15}$
71	0.04	$2 \cdot 10^{15}$
100	$2.4 \cdot 10^{-4}$	$1.1 \cdot 10^{13}$

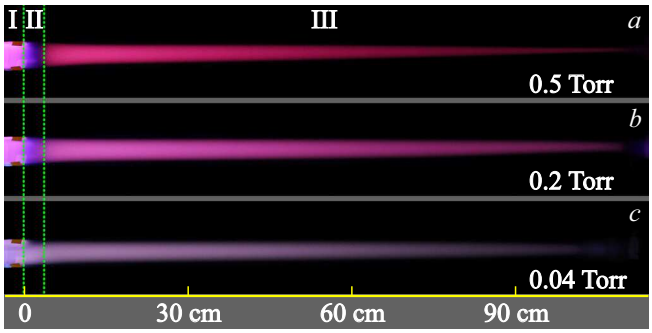

Figure 2. Photos of the integral glow of the streamer discharge plasma at air pressures $p = 0.5$ (a), 0.2 (it b) and 0.04 Torr (c). I — interelectrode region, II — near-electrode region, III — PDJ region. The voltage amplitude of the generator is 7 kV. The aperture of the camera lens is 5.6, Sensitivity ISO 3200. Exposure for 1050 (a) and for 2100 pulses (b, c).

the discharge plasma was carried out with a Canon 2000D digital camera (CANON).

Results

As already noted in the Introduction, although the initiation of red sprites usually occurs in the range of heights of 70–80 km from the Earth's surface, their radiation was recorded in the range of heights of 40–100 km, therefore, the most detailed studies of the radiation characteristics of the discharge were carried out at air pressures of 0.04, 0.2, 0.5, 1 and 3 Torr, which take place in the specified height range. The values of pressure and concentration of air particles for different heights above sea level are given in the table.

Data on the calculated values of particle concentrations, taking into account the non-monotonic change in air temperature as it moves away from the Earth's surface, were taken from the work [20].

The use of a generator with a voltage of 7 kV and a high pulse repetition rate made it possible to form a diffuse barrier discharge in a wide range of pressures. At high air pressure values (9 Torr and more), the discharge was ignited mainly in the part of the tube between the electrodes. With a decrease in p, the shape of the discharge changed, an ionization wave (streamer) appeared, which, like blue jets [10] and cylindrical sprites (column sprites [14]), had the shape of a PDJ. The length of the PDJ increased with a decrease in air pressure and (or) an increase in the voltage of the generator, and the PDJ could reach the opposite end of the tube. The mechanism of PDJ formation can only be streamer, since no additional electrode was installed on the right end of the tube. Accordingly, the PDJ propagated from the plasma formation zone of the barrier discharge between the electrodes due to the formation and propagation of ionization waves (streamers). This is confirmed by measuring the propagation velocities of the glow fronts propagating in opposite directions from the plasma formation zone between the ring electrodes installed in the middle part of the quartz tube [18,19]. So, at $p = 1.5$ the Torr value of this velocity reached 1.7 mm/ns, which corresponds to the velocity of the streamer front (ionization wave) under similar conditions [12,14]. Photos of the discharge plasma glow for three air pressure values at which the length of the PDJ exceeded 100 cm are shown in Fig. 2.

The pressure range $\Delta p = 0.04–3$ Torr corresponds to the range of heights at which both the red sprites themselves and the areas in which their color changed from red to blue were observed. We believe that the PDJ observed in laboratory conditions, like the sprites [1–15], are ionization waves. Let us describe their properties in detail. The greatest luminosity of the PDJ with a length of more than 100 cm took place at $p \sim 0.5$ Torr (Fig. 2, a).

An increase in pressure to 1 Torr led to a decrease in the length of the PDJ to ~ 50 cm, however, an increase in its luminosity occurred. The color of the PDJ when changing p from 3 to 0.2 Torr did not change significantly and was similar to the color of red sprites. Also, the color of the PDJ did not change along the jet as it moved away from the electrodes at a distance of 5 cm or more. The decrease in pressure under the conditions corresponding to the photographs in Fig. 2 did not significantly affect the length of the PDJ, but its color could change (Fig. 2, c).

At $p = 0.04$ Torr, which corresponds to the altitude above sea level ~ 71 km, the red component in the color of the PDJ has significantly decreased. A further decrease in the air pressure in the tube while maintaining the parameters of the generator voltage pulse led to the fact that the breakdown in the tube stopped, and, consequently, the PDJ was not formed. This experimental fact is explained by the growth of the breakdown voltage in accordance with the left branch of the Paschen curve. For the appearance of PDJ at small p, it was necessary to increase either the pulse amplitude of the generator voltage, or its duration and pulse repetition frequency. The change in the polarity of the generator did not have a noticeable effect on the length and color of the observed PDJ. Also, their length, color and shape were not affected by the orientation of the quartz tube in space. So, when turning it by 90° to the right or to the left, the PDJ spread up or down, respectively.

In order to determine the contribution of diffuse jets of bands and lines of various gases that make up the air to plasma radiation, its emission spectra were recorded during

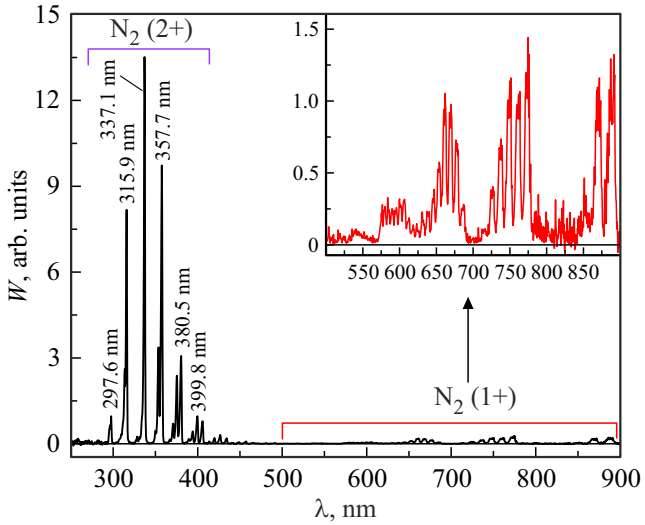

Figure 3. Spectral distribution of the energy density of the PDJ radiation at a distance of 21 cm from the electrode node in the range $\Delta\lambda = 250-900$ nm, as well as when using the GS-12 filter and increasing exposure in the range $\Delta\lambda = 500-900$ nm (inset). The transmission of the filter in the specified wavelength range is more than 90%. The filter absorbs radiation with a wavelength shorter than 500 nm. Air pressure $p = 1$ Torr.

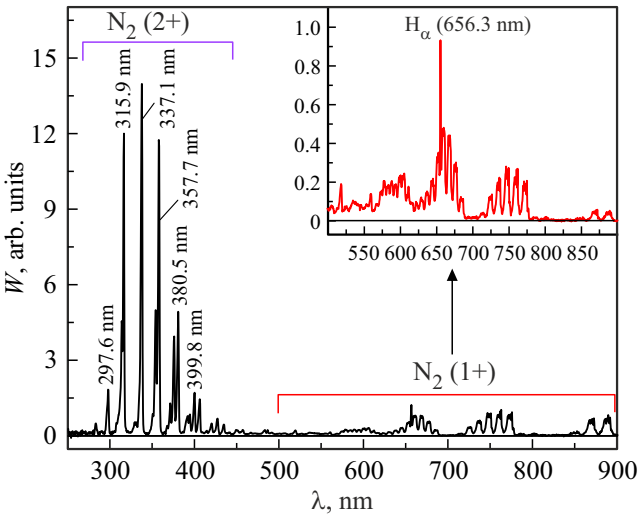

Figure 4. Spectral energy distribution of diffuse jet plasma radiation at a distance of 61 cm from the electrode node in the range $\Delta\lambda = 250-900$ nm and using the GS-12 filter and increasing exposure in the range $\Delta\lambda = 500-900$ nm (inset). The transmission of the filter in the specified wavelength range is more than 90%. The filter absorbs radiation with a wavelength shorter than 500 nm. $P = 0.2$ Torr.

experiments using a wide-range spectrometer. The light guide through which the radiation was transported to the input of the spectrometer was placed at the level of the central axis of the discharge tube. Spectra were recorded for three main discharge regions, which in most modes differed in color (regions I, II and III in Fig. 2). The discharge plasma emission spectra were recorded from the interelectrode region I, near the electrodes in the region II (at a distance of ~ 1 cm from the edge of the electrodes), and, in addition, the emission spectra of the PDJ were studied in detail at various distances — 11, 21, 41 and 61 cm from the edges of the electrodes (diffuse jet region III). As can be seen from Fig. 2, when moving away from the electrodes at a distance of several centimeters to tens of centimeters, the color of the PDJ does not change, so the entire jet was assigned to a single region III. The spectral distribution of the energy density of plasma radiation W from this region at a distance of 21 cm from the electrodes at an air pressure of 1 Torr is shown in Fig. 3. The same figure shows a part of the spectrum selected using the GS-12 filter, which transmits radiation in the range from 500 to 900 nm with a coefficient of more than 0.9.

It can be seen from the spectrogram in Fig. 3 that the highest spectral energy density in the wavelength range $\Delta\lambda = 250-900$ nm falls on separate bands of the second positive (2+) system of spectral transitions $C^3\Pi_u - B^3\Pi_g$ of molecular nitrogen N_2, and the maximum W is registered at $\lambda = 337.1$ nm (vibrational transition 0-0). The bands of the nitrogen system 1+ (transition system $B^3\Pi_g - A^3\Sigma_u^+$), whose detailed structure is shown in Fig. 3 (inset), account for an order of magnitude smaller fraction W. However, it is the radiation of these bands that determines the color of the PDJ under these excitation conditions, as well as the color of sprites during discharges in the upper layers of the Earth's atmosphere [2,4,9]. This can be explained by the greater width of the spectral region occupied by these bands. When the pressure decreases to 0.2 Torr, as can be seen from Fig. 2, *b*, the glow color of the discharge plasma changes somewhat, but the red hue dominates, as do the stripes of the systems 2+ and 1+ N_2 in the emission spectrum.

At pressures 1, 0.5 and 0.2 Torr with a distance from the electrodes at distances 11, 21, 41 and 61 cm, the emission spectra of the PDJ did not differ significantly from the one shown in Fig. 3. At a distance of 61 cm from the electrodes, the PDJ radiation spectrum for air pressure 0.2 Torr is shown in Fig. 4. As in Fig. 3, Fig. 4 shows the part of the spectrum selected using the GS-12 filter.

Even with a change in the air pressure in the tube, the selection of the region III from which the emission spectrum of the plasma of the diffuse jet was recorded did not have a noticeable effect on the spectral distribution of the radiation energy. A comparison of the spectra in Fig. 3 and 4 shows that they do not differ significantly, which means that the mechanism of formation of PDJ at its various points is preserved. This situation is realized during the propagation of ionization waves. However, a decrease in air pressure below $p = 0.2$ Torr led to the appearance of weak broadband radiation in the spectrum, apparently consisting of a large number of bands and lines in the range of 300–500 nm, and to a noticeable change in the color of the discharge plasma glow (Fig. 2, *with*). We also note

the appearance in the spectrum of a relatively strong line of atomic hydrogen H_α with a wavelength of $\lambda = 656.3$ nm (inset in Fig. 4).

With an increase in pressure to 3 Torr and a reduction in the length of the PDJ, the radiation spectrum was also similar to that shown in Fig. 3. At the same time, with increasing pressure, the ratio of the intensities of the bands of the system 2+ to the intensities of the bands of the system 1+ increased in favor of the system 2+, but the color of the PDJ in the photos and visually was the same as at a pressure of 0.5 Torr.

It is known [2,21], that part of the sprites at a height of 40–50 km at pressures 0.5–3 Torr changes red to blue. A change in the color and intensity of discharge plasma radiation at air pressures 0.5 and 0.2 Torr is observed in these experiments at electrodes in the region II. At a distance of ~ 1 cm from the electrodes, the discharge color becomes darker, and a blue area also appears. The width of the dark area following the blue one to the right of the electrodes depends on the air pressure. The radiation spectra from the II region, as well as its color, undergo a significant change in relation to the spectra of diffuse jets from the III region. At the same time, the difference in the spectra becomes more apparent with a decrease in gas pressure. At $p = 0.2$ Torr in the emission spectrum recorded from the near-electrode region, the radiation intensity of the bands of the first negative (1–; $B^2\Sigma_u^+ - X^2\Sigma_g^+$) increases significantly systems of molecular nitrogen ion N_2^+ (lines with wavelengths 391.4, 427.8 and 470.9 nm, Fig. 5).

In addition, the spectrogram (Fig. 5) shows intense molecular bands and atomic lines that are absent in the emission spectrum of the PDJ (region III). Thus, the bands belonging to the Angstrom system of the CO molecule ($B^2\Sigma^+ - A^1\Pi$; $\lambda = 282$, 288.2, 289.7 nm), the first

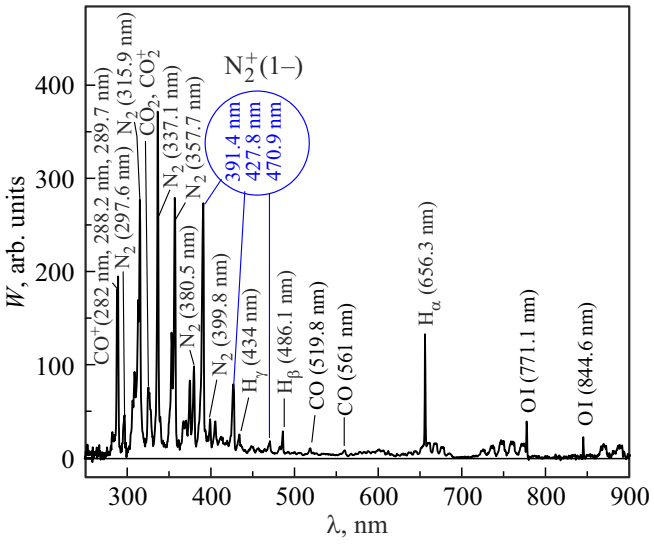

Figure 5. Spectral distribution of plasma radiation energy in the near-electrode region II, at a distance of 1 cm from the edge of the electrodes. Air pressure in the tube $p = 0.2$ Torr.

negative system of the molecular CO^+ ion ($B^2\Sigma^+ - X^2\Sigma^+$; $\lambda = 519.8$, 561 nm), as well as atomic hydrogen lines of the series Balmer H_α ($\lambda = 656.3$ nm), H_β ($\lambda = 486.1$ nm), H_γ ($\lambda = 434$ nm) and oxygen O I ($\lambda = 777.1$ nm) and O I ($\lambda = 844.6$ nm). In addition, the sequence of low-intensity bands occurring in the wavelength range $\Delta\lambda = 320–330$ nm can be attributed to the spectral transitions formed by the molecule CO_2 and the molecular ion CO_2^+, and the bands interspersed with the bands of the system 1+ N_2 — to the bands of molecular hydrogen. However, this statement requires more thorough verification in experiments using equipment with a higher spectral resolution.

Nevertheless, the presence of the above-mentioned bands of carbon monoxide and carbon dioxide in the emission spectrum is explained by the presence of these gases in the air in the form of an impurity, which can also include water vapor, which is identified by the presence of the OH molecule band ($A^2\Sigma^+ - X^2\Pi$) in the range $\Delta\lambda = 306–309$ nm and is clearly manifested in experimentally recorded plasma emission spectra from the near-electrode (II) and interelectrode (I) regions. The presence of the above-listed bands and lines in these discharge regions is fully explained by an increase in the reduced electric field strength E/N in them (E — electric field strength, N — particle concentration) and, consequently, the electronic temperature T_e, which it has a positive effect in terms of dissociation of molecules (for example, CO_2, O_2, H_2O and H_2 with subsequent excitation of their atomic states, as well as molecular fragments), as, for example, in the case of the molecular ion CO^+.

The highest spectral energy density of radiation at low pressures can be achieved at $\lambda = 391.4$ nm of a molecular ion. In Fig. 5, the intensity of radiation at the specified wavelength is inferior in intensity to only two bands ($\lambda = 337.1$ and 357.7 nm) systems 2+N_2, and at a pressure of 0.04 its Torr W was the largest in the range $\Delta\lambda = 200–1100$ nm. It should also be noted that with a decrease in air pressure in the regions I and II, there is an increase in radiation in the wavelength range from 300 to 500 nm, which has the form of a broadband continuum.

The radiation spectrum of the discharge plasma and the region between the electrodes (region I) was similar to the radiation spectrum at a distance of 1 cm from them. However, the spectral energy density of the radiation of the 1– system, the CO^+ and CO bands, as well as the lines of atomic hydrogen and oxygen with respect to the W bands of the 2+ and 1+ systems has increased. Moreover, this difference in the values of W increased with decreasing pressure (Fig. 6).

In this case, the highest spectral energy density of radiation in the range $\Delta\lambda = 200–1100$ nm, which in the region I at a pressure of 0.2 Torr took place for the band of the system 1–N_2^+ with $\lambda = 391.4$ nm, has been observed for other spectral components. Thus, with a decrease in air pressure to 0.04 Torr in the radiation spectrum from the region between the electrodes, the largest W was the

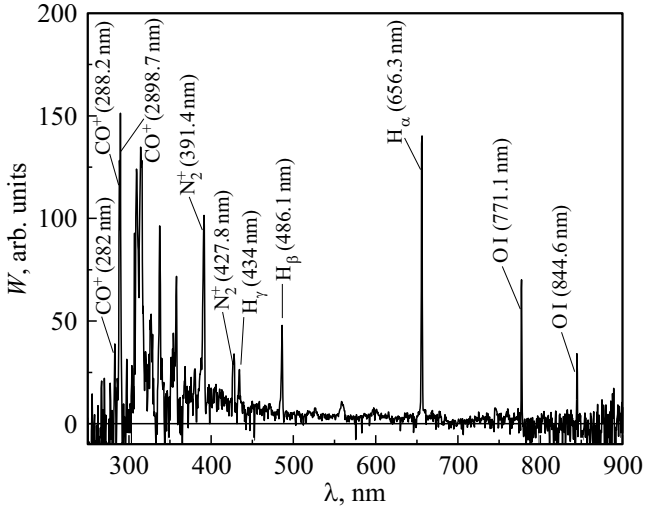

Figure 6. Spectral distribution of plasma radiation energy from the region I between the electrodes. Air pressure in the tube $p = 0.04$ Torr.

atomic hydrogen line H_α with $\lambda = 656.3$ nm and the carbon monoxide ion band CO^+ with $\lambda = 289.7$ nm.

Thus, it was experimentally established that in a wide range of air pressures, the glow color of the discharge plasma in the jets remains red and is determined by the radiation of the system $1+$ N_2. As for the near-electrode and interelectrode regions, where E/N is much higher, the type of emission spectra of the discharge plasma is noticeably different for them. It is also worth noting the significant influence of pressure p (in particular, its decrease) on the type of spectral distribution of plasma radiation energy from the regions I and II.

Discussion of the results

First, we note that a diffuse discharge (nonequilibrium low-temperature plasma) was formed on the created experimental setup. The diffuse form of the discharge follows from its morphology and the spectral composition of plasma radiation in a wide wavelength range, in which the radiation of the $2+$ molecular nitrogen system dominates in intensity. During spark discharges in air and other gases, bright channels are visually observed, and broadband radiation is recorded in the radiation spectrum, resembling Planck radiation in shape, against which ion lines [22] appear. With diffuse discharge in air and its mixtures with helium and argon, including when excited by a barrier discharge [23], the bands of the system $2+$ have the greatest intensity. In addition, the estimates carried out by the Boltzmann method [24] for the rotational distribution of the nitrogen band with $\lambda = 337.1$ nm show that the temperature of the heavy plasma component T_g under these excitation conditions, depending on the location in the discharge tube, varies within 330–400 K. The lowest gas temperature occurs in a diffuse jet, increasing in the near-electrode and interelectrode regions.

The experiments have shown that three main areas can be distinguished in the glow of the plasma of the discharge under study. In all regions at pressures of 9–0.04 Torr bright channels were absent — both in the region of the barrier discharge between the electrodes (discharge region I) and in the other two regions, which were located at small (II) and large (III) distances from the electrodes. Part of the II region remains dark in a wide range of conditions and smoothly passes into the region of the diffuse jet III. At pressures above 0.04 the Torr part of the region II has a blue color, which can be explained by the intense radiation in this region of the molecular nitrogen ion and atomic hydrogen, as well as bands of molecules and ions of carbon monoxide and dioxide (reliably identified by other spectral components), which are characteristic of this spectral region, but difficult to distinguish with the available spectral equipment. At a pressure of 0.04 Torr, the color of the regions II and III was the same (Fig. 2, *c*).

The greatest interest from the point of view of modeling atmospheric sprites is the region III, which in a wide range of pressures is a red PDJ. We believe that the PDJ formed in the III region is a consequence of the sequential propagation of ionization waves (streamers) formed in the zone of the electrode node in it. The length of the PDJ depends on the air pressure in the tube and the voltage applied to the electrodes. In addition, the proof of the formation of streamers, which have the form of jets of predominantly red color, is their velocity, which is centimeters per nanosecond [18,19], and their propagation over long distances from the electrodes observed in this work.

From discharge plasma emission spectra recorded from the regions I and II, it follows that W by $\lambda = 391.4$ and 427.8 nm of ion N_2^+ it increases significantly, and, in addition, atomic lines and molecular bands of air and water vapor components appear, which, in turn, indicates the possibility of their effective dissociation, ionization and excitation in these zones.. Accordingly, the reduced electric field strength E/N and, consequently, the electron temperature T_e in these discharge regions should be higher than in the region III. This statement is confirmed by the estimates of E/N by the method based on the measurement of the ratio of $R_{391/337}$ and $R_{391/394}$ of the peak radiation intensities of the bands of the molecular nitrogen ion N_2^+ ($lambda = 391.4$ nm) and nitrogen molecules N_2 ($lambda = 337.1$ and 394.3 nm) [25]. In this case, using an HR4000 spectrometer (OceanOptics Inc.) with known spectral sensitivity and hardware function ~ 0.2 nm, an emission spectrum in the range $\Delta\lambda = 300–400$ nm was recorded from various zones of the discharge tube, based on which the $R_{391/337}$ and $R_{391/394}$ and were compared with the values of E/N. Estimates show that as we move from the end of the diffuse jet to the interelectrode region, the reduced electric voltage changes from ~ 250 to ~ 1000 Td, which clearly indicates an increase in T_e in the I and II

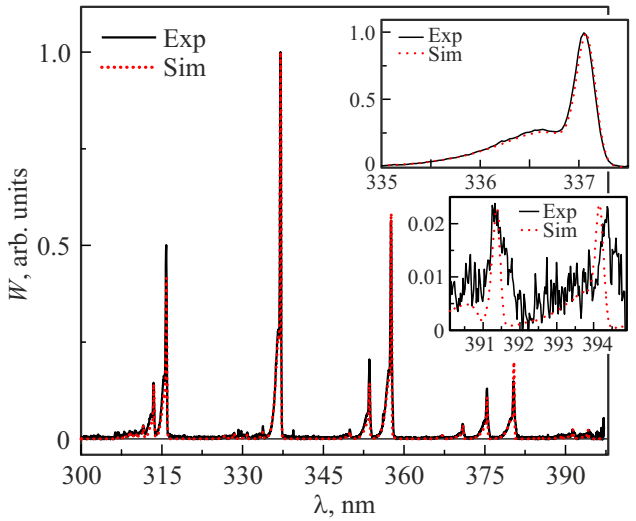

Figure 7. Experimental (Exp) and calculated (Sim) using the SPECAIR code, emission spectra of diffuse jet plasma from the region III at a distance of 41 cm from the electrodes in the wavelength range $\Delta\lambda = 300-400$ nm. Air pressure in the tube $p = 0.2$ Torr. The electronic T_e, vibrational T_v, rotational T_r and gas T_g temperatures measured in the experiment were 3.7 eV, 3000 K, 350 K and 380 K, respectively.

regions. So, within the PDJ, T_e varies in the range 2−4.5 eV. It is worth noting that the values of electron and gas temperatures measured in the experiment by the above methods were used for modeling using the SPECAIR [26] code of plasma emission spectra in the region of propagation of ionization waves under experimental conditions. The estimated values of temperatures and the reduced electric field strength confirm the conclusion about the propagation of ionization waves in the region III. For example, Fig. 7 shows the spectrum of plasma radiation in a diffuse jet at a distance of 41 cm from the edge of the electrodes at a pressure of 0.2 Torr.

The experimentally obtained and simulated radiation spectra for this discharge zone are in good agreement. As for the near-electrode and interelectrode regions, in this case, the operability of the method for determining T_e [27] requires verification, which will require additional research. In this paper, calculations of plasma parameters using the SPECAIR code for the discharge region between the electrodes and at the electrodes were not carried out. More detailed measurements of the values of T_e and other basic plasma parameters under these conditions are the subject of independent research and a separate publication in which the time course of voltage, current and optical signals will be given.

The color change of sprites from red to blue occurs at air pressures ≥ 0.5 Torr [2,21]. In the installation presented in this paper, the region of propagation of ionization waves in the studied pressure range had a red color, which was replaced by blue in the near-electrode region II. We also note that the color of the sprites in the photographs presented in the literature and the Internet remains red at altitudes that correspond to pressures 0.5−3 Torr [28]. It can be assumed that the change in the color of sprites as they approach the Earth is primarily due to a change in the electric field in this area. As shown earlier [2,3,12,13], the appearance of red sprites is usually caused by a preliminary breakdown between positively charged clouds and the Earth's surface. Due to the return strike, lightning carries a negative charge to the top of the clouds and initiates the spread of sprites downwards. The electric field changes rapidly after the lightning current flows. This, we believe, can lead, at maximum values of the reduced electric field E/N, to a change in the color of the sprite from red to cyan/blue. Further, due to a rapid decrease in E/N, as well as due to an increase in air pressure when approaching the Ground, the lower part of the sprite stops and fades. Based on the observed difference in the color of the discharge regions II and III, the change in the color of giant sprites from red to blue when approaching the Earth can be explained by an increase in the reduced electric field strength in this region. At the minimum heights of the sprite, the color of its glow is also influenced by an increase in air pressure and the associated increase in W bands of the nitrogen system 2+ compared to the bands of the system 1+.

The highest values of E/N are realized in the interelectrode gap (region I), which follows from the high values of W lines of hydrogen, oxygen and molecular bands of air impurities (Fig. 6), as well as from the design of this installation. The largest specific energy deposits are also realized in the region I. This leads to the dissociation of molecules that make up the air, including water vapor. We note that in the work [29], when excited by a low-pressure air glow discharge, the effect of its humidity on the radiation spectrum at $p = 7$ Torr was not recorded, and the atomic hydrogen line H_α at $p = 7$ Torr had a low intensity.

The change in the discharge color in all regions (Fig. 2, *c*) at low air pressures is associated with an increase in E/N due to a decrease in the particle concentration of N and, accordingly, the average electron temperature. Under these conditions, the rate of dissociation of molecules that are part of the air and adsorbed on the walls of the chamber increases, as well as their excitation and ionization. The number of emitting atoms and ions increases, which leads to the registration of a wide spectrum of plasma radiation in the wavelength range $\Delta\lambda = 300-500$ nm. Due to the appearance of a large number of new lines and stripes, as well as due to the increase in T_e, the stripes of the nitrogen 1+ system cease to determine the color of the discharge. During the verification experiment and the replacement of air with high purity nitrogen (99.999%), the bands of nitrogen systems 2+, 1+ and 1− remain in the radiation spectrum, and their behavior with pressure changes is preserved. However, the lines of atomic hydrogen and oxygen, as well as the bands of molecules and ions of carbon monoxide and carbon dioxide disappear.

Conclusion

Studies of the radiation spectra of a streamer discharge initiated by a barrier pulse-periodic discharge at atmospheric air pressures 0.01−10 Torr, have shown that the color of the radiation can both correspond to the observed and photographed radiation of red sprites, and vary depending on the reduced electric field strength and pressure. With an increase in the reduced electric field strength, along with the radiation of the first and second positive nitrogen systems, the bands of the first negative molecular nitrogen ion system begin to make a noticeable contribution to the spectral distribution of the radiation energy, and the highest spectral energy density in the wavelength range 200−1100 nm can be registered at $\lambda = 391.4$ nm. A further increase in the reduced electric field strength due to a decrease in air pressure leads to a change in the color of the discharge and the type of emission spectra of the discharge plasma. Thus, at a pressure of 0.04 Torr in the interelectrode region, the highest plasma radiation power is recorded on the atomic hydrogen line 656.3 nm. In addition, an increase in the reduced electric field strength and a decrease in air pressure give an increase in the radiation intensity in the range of 300−700 nm. The color of the observed and photographed radiation under these conditions becomes close to white.

An important feature of the change in the color and spectrum of the discharge is recorded at short distances from the electrodes in the region of increased values of the reduced electric field strength. The discharge color visually and in photographs turns blue/cyan, and intense bands of molecular nitrogen ion (391.4 and 427.8 nm) and lines of hydrogen atoms (434 and 486.1 nm) appear in the spectrum. As you know, some sprites also change color from red to blue when their front approaches the upper boundary of the clouds.

We assume that the results obtained and the created installation will be useful for studying red sprites and other TLP.

Acknowledgments

The authors express their gratitude to D.S. Pechenitsin for the development of a pulse-periodic voltage source.

Funding

This study was carried out with the financial support of the Ministry of Science and Higher Education of the Russian Federation under the Agreement No.075-15-2021-1026 dated November 15, 2021.

Conflict of interest

The authors declare that they have no conflict of interest.

References

[1] C.J. Rodger. Rev. Geophys., **37** (3), 317 (1999).
[2] V.P. Pasko. Plasma sources science and technology, **16**, S13 (2007). DOI: 10.1088/0963-0252/16/1/S02
[3] J. Qin, V.P. Pasko, M.G. McHarg, H.C. Stenbaek-Nielsen. Nature commun., **5** (1), 1 (2014). DOI: 10.1038/ncomms4740
[4] C.L. Kuo, E. Williams, T. Adachi, K. Ihaddadene, S. Celestin, Y. Takahashi, R.R. Hsu, H.U. Frey, S.B. Mende. Front. Earth Sci., **9**, 1102 (2021). DOI: 10.3389/feart.2021.687989
[5] S. Nnadih, M. Kosch, J. Mlynarczyk. J. Atmosph. Solar-Terr. Phys., **225**, 105760 (2021). DOI: 10.1016/j.jastp.2021.105760
[6] M. Singh, P.K. Sharma, P.P. Pathak. J. Electromag. Analys. Appl., **14** (3), 31 (2022). DOI: 10.4236/jemaa.2022.143003
[7] D.D. Sentman, E.M. Wescott. Geophys. Res. Lett., **20** (24), 2857 (1993).
[8] D.D. Sentman, E.M. Wescott, D.L. Osborne, D.L. Hampton, M.J. Heavner. Geophys. Res. Lett., **22** (10), 1205 (1995).
[9] G.K. Garipov, B.A. Khrenov, P.A. Klimov, V.V. Klimenko, E.A. Mareev, O. Martines, E. Mendoza, V.S. Morozenko, M.I. Panasyuk, I.H. Park, E. Ponce, L. Rivera, H. Salazar, V.I. Tulupov, N.N. Vedenkin, I.V. Yashin. J. Geophys. Res.: Atmosph., **118** (2), 370 (2013). DOI: 10.1029/2012JD017501
[10] T. Neubert, N. Østgaard, V. Reglero, O. Chanrion, C.A. Oxborrow, A. Orr, M. Tacconi, O. Hartnack, D.D. Bhander. Space Sci. Rev., **215** (2), 1 (2019). DOI: 10.1007/s11214-019-0592-z
[11] R.A. Marshall, U.S. Inan. Radio Science, **41**, RS6S43 (2006). DOI: 10.1029/2005RS003353
[12] T. Kanmae, H.C. Stenbaek-Nielsen, M.G. McHarg, R.K. Haaland. J. Phys. D., **45** (27), 275203 (2012). DOI: 10.1088/0022-3727/45/27/275203
[13] U. Ebert, S. Nijdam, C. Li, A. Luque, T. Briels, E. van Veldhuizen. J. Geophys. Res.: Space Phys., **115**, A00E43 (2010). DOI: 10.1029/2009JA014867
[14] J. Qin, S. Celestin, V.P. Pasko, S.A. Cummer, M.G. McHarg, H.C. Stenbaek-Nielsen. Geophys. Res. Lett., **40** (17), 4777 (2013). DOI: 10.1002/grl.50910
[15] E. Williams, M. Valente, E. Gerken, R. Golka. *Sprites, Elves and Intense Lightning Discharges* (Springer, Dordrecht. 2006), p. 237–251.
[16] V.F. Tarasenko, E.A. Sosnin, V.S. Skakun, V.A. Panarin, M.V. Trigub, G.S. Evtushenko. Physics of Plasmas, **24** (4), 043514 (2017). DOI: 10.1063/1.4981385
[17] V.S. Kuznetsov, E.A. Sosnin, V.A. Panarin, V.S. Skakun, V.F. Tarasenko. Opt. Spectrosc., **125** (3), 324 (2018). DOI: 10.1134/S0030400X18090175.
[18] V. Tarasenko, N. Vinogradov, E. Baksht, D. Sorokin. J. Atmosph. Sci. Res., **05** (03), 26 (2022). https://doi.org/10.30564/jasr.v5i3.4858
[19] E.H. Baksht, N.P. Vinogradov, V.F. Tarasenko. Optika atmosfery i okeana, **35** (9), 777 (2022). (in Russian). DOI: 10.15372/AOO20220911.
[20] E.E. Remsberg, B.T. Marshall, M. Garcia-Comas, D. Krueger, G.S. Lingenfelser, J. Martin-Torres, M.G. Mlynczak, J.M. Russell III, A.K. Smith, Y. Zhao, C. Brown. J. Geophys. Res.: Atmosph., **113**, D17101 (2008). DOI: 10.1029/2008JD010013
[21] E.R. Williams. Phys. Today, **54** (11), 41 (2001).
[22] T. Shao, V.F. Tarasenko, C. Zhang, M.I. Lomaev, D.A. Sorokin, P. Yan, A.V. Kozyrev, E.Kh. Baksht. J. Appl. Phys., **111** (2), 023304 (2012). DOI: 10.1063/1.3677951

[23] A.A. Heneral. Opt. Spectrosc., **127** (5), 778 (2019). DOI: 10.1134/S0030400X19110092.
[24] D.M. Philips. J. Phys. D., **9** (3) 507 (1975). DOI: 10.1088/0022-3727/9/3/017
[25] P. Paris, M. Aints, F. Valk, T. Plank, A. Haljaste, K.V. Kozlov, H.-E. Wagner. J. Phys. D., **38** (21), 3894 (2005). DOI: 10.1088/0022-3727/38/21/010
[26] C.O. Laux. *Radiation and Nonequilibrium Collisional-Radiative Models. In: Physico-Chemical of High Enthalpy and Plasma Flows.* von Karman Institute Lecture Series 2002–2007. Fletcher D, Carbonnier J-M, Sarma GSR, Magin T. Eds. (Rhode Saint Genése, Belgium, 2002).
[27] N. Britun, M. Gaillard, A. Ricard, Y.M. Kim, K.S. Kim, J.G. Han. J. Phys. D., **40** (4) 1022 (2007). DOI: 10.1088/0022-3727/40/4/016
[28] Facebook. Available online: http://www.facebook.com/frankie.lucena.1 (accessed on 01.11.2021).
[29] Y. Goto, Y. Ohba, K. Narita. J. Atmosph. Electr., **27** (2), 105 (2007).